Int. J. Heat Mass Transfer. Vol. 34, No. 4/5, pp. 993–1001, 1991
Printed in Great Britain

0017–9310/91 $3.00 + 0.00

Critical heat flux of counter-flow boiling in a uniformly heated vertical tube with a closed bottom

Y. KATTO and T. HIRAO
Department of Mechanical Engineering, Nihon University, Kanda-Surugadai, Chiyoda-ku, Tokyo 101, Japan

(*Received* 28 *March* 1990)

Abstract—An experimental study is carried out on the critical heat flux (CHF) of counter-flow boiling in a uniformly heated vertical tube which is open to an upper, large liquid reservoir and closed at the bottom end. CHF characteristics which are quite different from those of CHF in the ordinary boiling system are revealed, particularly the matters such as the location to initiate CHF in the tube, a noticeable time-lag and a subsequent period for falling of local wall temperature just before the onset of CHF, and the complicated and comparatively slow variation of local wall temperature after the onset of CHF. Then a physical model capable of explaining such peculiar phenomena through the behavior of vapor and liquid in a heated tube is discussed.

1. INTRODUCTION

MANY experiments relating to the performance of heat pipes and gas turbine blade cooling have so far been made for the critical heat flux (CHF) of counter-flow boiling in a heated vertical tube closed at the bottom end as shown in Figs. 1(a) and (b). For some of the experimental studies, the main experimental conditions are listed in Table 1, together with information as to the number of thermocouples placed along the length of the tube, the location of the onset of CHF in the tube, and the mode of temperature variation.

Among the experimental studies listed in Table 1, comparatively recent studies [5–9] provide us with the following information as to the limiting phenomena observed in the boiling system of Fig. 1(a).

First, Harada *et al.* [5] observed a hammering sound accompanied by irregular variation of wall temperature with time, and assumed it to be a limiting state caused by a sort of flooding. In addition, their boiling system was found to become uncontrollable at a liquid charge of $F_c = 0.17$, and they attributed it to the fall of a mass of liquid accumulated in the upper cooling section into the lower heated section.

Imura *et al.* [6] studied the effect of the liquid charge F_c on the magnitude of CHF q_c over the range of $F_c = 0.04$–1.0, leading to the following classification of three characteristic regimes: the regime of small F_c where q_c increased with F_c, then that of middle F_c where q_c was constant independent of F_c, and finally that of large F_c where a periodic burst of boiling and noise were observed. They then assumed the dryout of the liquid film under the situation of Fig. 2(a) for the first regime, and burnout under the situation of Fig. 2(b) for the second regime.

Fukano *et al.* [7] showed three different types of graphs of wall temperature excursion. The first is the oscillation of wall temperature (and pressure in the tube) with a period of about 240 s and an amplitude of about 200°C, which they assumed, under the situation of Fig. 2(c), to occur through a cyclic phenomenon consisting of the accumulation of liquid by flooding in the upper cooling section and the extension of the dryout area above the free surface of the liquid pool. Then, they attributed the second type of temperature excursion to the dryout of liquid film appearing at small liquid charges, and the third type to the CHF of DNB type occurring in the liquid pool at large liquid charges.

Reference [8], reporting experiments in the range of tube diameter $d = 13.8$–23.0 mm and liquid charge $F_c = 0.25$–0.50, has disclosed that the above-mentioned temperature oscillation of ref. [7] can occur only near $F_c = 0.33$. Then, in a subsequent study [9], derivation of a generalized correlation of the CHF data obtained for $F_c = 0.10$–0.50 was attempted without distinction of the type of temperature excursion.

On the other hand, as for the boiling system of Fig. 1(b), Barnard *et al.* [10] reported data associated with the location to initiate temperature excursion for R-113 at atmospheric pressure (vapor/liquid density ratio $\rho_v/\rho_L = 0.00495$). If they are represented in a generalized form, it results in Fig. 3 where L_c/L designates the relative distance of the CHF onset point measured from the bottom. Then, Barnard *et al.* assumed the state of Fig. 4(a) to appear in longer tubes (say, $L/d > 70$), where dryout would be initiated at the bottom end.

As for analytical studies, there are those made by Dobran [13], Reed and Tien [14], and Casarosa and Dobran [15], respectively. Dealing with the system of Fig. 1(a), these authors analyzed the circulation of fluid and its stability based on a two-phase model such as Fig. 2(c), and discussed the occurrence of flooding and dryout.

Meanwhile, flooding has been regarded by many

NOMENCLATURE

d	i.d. of heated tube	P	pressure
F_c	liquid charge (volume fraction in heated tube) in the case of Fig. 1(a)	q	heat flux
		q_c	critical heat flux
g	gravitational acceleration	T_s	saturation temperature
H_{fg}	latent heat of evaporation	z	axial distance measured from the bottom.
j_L	superficial velocity of liquid, equation (2)		
j_v	superficial velocity of vapor, equation (2)		
L	length of heated tube	Greek symbols	
L_c	location of CHF onset measured from the bottom	σ	surface tension
		ρ_L	density of liquid
L_w	liquid level in reservoir	ρ_v	density of vapor.

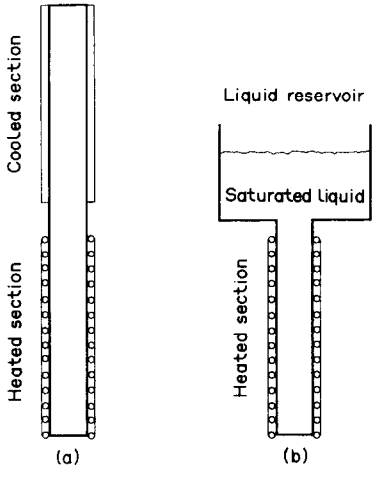

FIG. 1. (a) Closed two-phase thermosyphon. (b) Vertical tube with a liquid reservoir and a closed bottom.

investigators as a trigger of the CHF phenomenon in the present boiling system. Flooding itself is a phenomenon with very complicated aspects (cf. ref. [16] for example), accordingly it is undesirable to deal with it easily. However, since the effect of flooding will be considered later, a few correlations of CHF based on the concept of flooding are examined here.

First, with respect to the flooding which occurs in an annular counter-current flow of gas and liquid, Wallis [17] gave a well-known empirical equation:

$$(j_v^*)^{1/2}+(j_L^*)^{1/2}=C_w \tag{1}$$

with the following j_v^* and j_L^*:

$$j_v^*=j_v\rho_v^{1/2}/[g(\rho_L-\rho_v)d]^{1/2}$$

$$j_L^*=j_L\rho_L^{1/2}/[g(\rho_L-\rho_v)d]^{1/2}$$

where j_v and j_L are superficial velocities of gas and liquid, respectively; ρ_v and ρ_L are the densities of gas and liquid; g the gravitational acceleration; d the i.d. of the tube; and C_w a constant (say, 0.725–1.0).

In the case of applying equation (1) to the CHF of boiling in a heated tube closed at the bottom, the magnitudes of j_v and j_L at the top end of the heated tube are usually employed, and hence the following combined equation of continuity and energy holds at the critical heat flux q_c:

$$j_v\rho_v(\pi d^2/4)=j_L\rho_L(\pi d^2/4)=q_c\pi dL/H_{fg} \tag{2}$$

where H_{fg} is the latent heat of evaporation. Substituting j_v and j_L of equation (2) into equation (1) gives the following correlation of q_c:

$$\frac{q_c}{\rho_v H_{fg}}\Bigg/\left[\frac{g(\rho_L-\rho_v)d}{\rho_v}\right]^{1/2}=\frac{C_w^2}{4}\,\frac{1}{[1+(\rho_v/\rho_L)^{1/4}]^2(L/d)} \tag{3}$$

Among the studies cited in Table 1, Sakhuja [2] and Suematsu *et al.* [3] reported the agreement of his or their own data with equation (3), while Barnard *et al.* [10] reported a tendency of their own data to approach equation (3) with increasing the tube length in the range of $L/d<70$.

On the other hand, Harada *et al.* [5] posed a question to the general applicability of equation (3) according to the result of comparing their own data with equation (3). Diehl and Koppany [18], and Bezrodnyi [19], assuming the situation of flooding, proposed correlations of different types from equation (3), respectively. Besides, Nejat [11] gave the following empirical modification for C_w^2 on the right-hand side of equation (3) based on his own data:

$$C_w^2=0.36(L/d)^{0.1}. \tag{4}$$

Meanwhile, Tien and Chung [20] extended Kutateladze's criterion for the onset of flooding to give

$$K_v^{1/2}+K_L^{1/2}=c_k \tag{5}$$

with the following K_v and K_L:

$$K_v=j_v\rho_v^{1/2}/[\sigma g(\rho_L-\rho_v)]^{1/4}$$

$$K_L=j_L\rho_L^{1/2}/[\sigma g(\rho_L-\rho_V)]^{1/4}$$

where σ is the surface tension, and c_k is a constant ($c_k^2=3.2$). In this case, substituting j_v and j_L of equa-

Table 1. Experiments of CHF of counter-flow boiling in a vertical tube closed at the bottom end

Type Fig. 1	Authors	Fluid	Tube material	Heating	d (mm)	L/d	No. of TC†	CHF onset location	CHF wall temperature	Ref.
(a)	Cohen and Bayley	Four kinds	Copper	Electric wire	6.4–38.1	4.0–24.0	5	Bottom end	Sharp rise	[1]
(a)	Sakhuja	Two kinds	Carbon steel	Electric wire	17.3–23.6	2.1–7.4	3	Top end	Sharp rise	[2]
(a)	Suematsu *et al.*	Dowtherm-A	Stainless steel	Furnace	15.7–16.7	13.2–17.2	2	—	—	[3]
(a)	Fukui *et al.*	R-113	Aluminum	Electric wire	6.3–21.0	9.5–31.7	2	—	Sharp rise	[4]
(a)	Harada *et al.*	Water	Carbon steel	Steam	45.0	76.7	3	—	Unstable	[5]
(a)	Imura *et al.*	Three kinds	Brass	Electric wire	13.1–19.4	7.7–23.0	4	Lower half	Sharp rise	[6]
(a)	Fukano *et al.*	Two kinds	Copper	Electric wire	9.5–20.9	18.9–21.9	5	—	Three types	[7]
(a)	Fukano *et al.*	Methanol	Copper	Electric wire	13.8–23.0	20.2–32.6	5	—	Three types	[8]
(a)	Fukano *et al.*	Three kinds	Copper	Electric wire	13.8–22.0	20.9–61.6	5	—	Sharp rise	[9]
(b)	Barnard *et al.*	R-113	Stainless steel	Direct a.c.	17.2	8.7–58.1	5–7	See Fig. 3	Sharp rise	[10]
(b)	Nejat	Four kinds	Copper	Direct d.c.	8.0–14.0	10.7–18.4	4	—	—	[11]
(b)	Smirnov	Water	—	Electrical	6.0–23.0	20.0–400.0	—	Bottom third	—	[12]
(b)	Present work	Water	Stainless steel	Direct a.c.	8.0–10.0	30.0–112.5	11–17	See Fig. 9	See Fig. 7	—

† TC, thermocouple.

tion (2) into equation (5) gives the following correlation of q_c:

$$\frac{q_c}{\rho_v H_{fg}}\Big/\left[\frac{\sigma g(\rho_L-\rho_v)}{\rho_v^2}\right]^{1/4}=\frac{c_k^2}{4}\frac{1}{[1+(\rho_v/\rho_L)^{1/4}]^2(L/d)}. \tag{6}$$

In addition, Imura *et al.* [6] assuming the state of Fig. 2(b) which is independent of flooding, derived the following empirical correlation based on dimensional analysis:

$$\frac{q_c}{\rho_v H_{fg}}\Big/\left[\frac{\sigma g(\rho_L-\rho_v)}{\rho_v^2}\right]^{1/4}=0.16\frac{1}{(L/d)(\rho_v/\rho_L)^{0.13}}. \tag{7}$$

However, it is of interest to note that the right-hand side of equation (7) has a magnitude as much as about 66% of that of equation (6) throughout the normal range of the vapor/liquid density ratio $\rho_v/\rho_L = 0.000624$–0.15 [21]. This means that equation (7) is nearly equivalent to equation (6) except for the value of the constant.

Now, the studies mentioned so far have revealed various aspects of CHF in the present boiling system, but they are inconsistent in some key points (see Table 1, for example), and it is rather difficult to have a coherent image for the situation at the onset of CHF. In addition, clarifying the mechanism to generate CHF in this special counter-flow boiling system must be very useful to promote a general understanding of the phenomenon of CHF. For such reasons, the present study has been conducted employing a system of Fig. 1(b) with a uniformly heated tube, free from various secondary phenomena involved in a closed-space system of Fig. 1(a).

2. EXPERIMENTAL APPARATUS AND TEST RANGE

The experimental apparatus, which is illustrated schematically in Fig. 5, consists of a liquid reservoir, a test-tube, and a measuring system.

The liquid reservoir 200 mm in internal diameter and 610 mm in internal height, with auxiliary heaters and cooling coils in it, can keep a liquid at a prescribed saturation temperature and pressure. It has also a level gauge capable of measuring the liquid level even at high pressures.

The test-tube, a stainless steel tube with a wall thickness of 1 mm, is heated uniformly by a direct a.c. current of low voltage. Both ends of the tube are connected with electrodes, respectively, in such a way as illustrated in Fig. 6 (which exemplifies the upper end) so as to enable the reduction of contact resistance as well as an exchange of test-tubes of different lengths and diameters.

The local temperature of the test-tube is measured by chromel–alumel thermocouples spot welded to the tube wall at equal intervals (total of 11–17 points

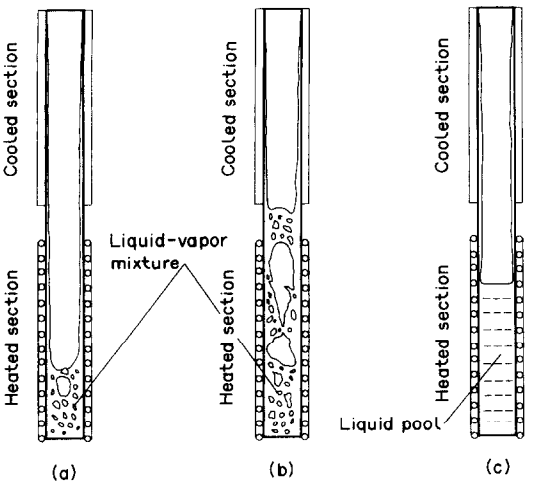

FIG. 2. State of liquid and vapor in a closed two-phase thermosyphon.

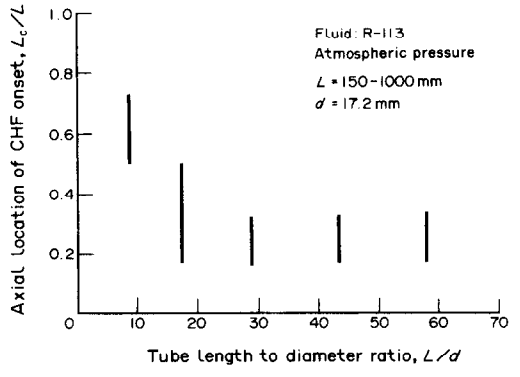

FIG. 3. Location of the onset of temperature excursion [10].

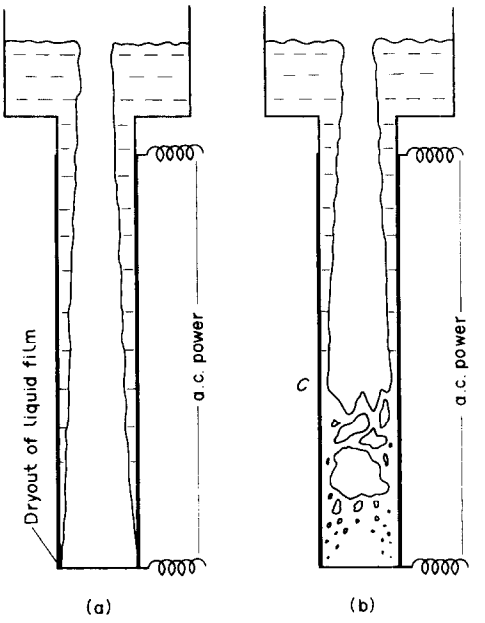

FIG. 4. State of liquid and vapor in a heated tube: (a) model of Barnard *et al.* [10] for long tubes; (b) model of the present work.

according to the tube length). Electric power input to the tube is measured by means of a voltmeter and a shunt, while a circuit breaker cuts off automatically the input current when the highest local temperature of the test-tube exceeds a prescribed limiting value. All the data of temperature and power input are recorded continuously by a computer through a scanner and a digital multimeter.

In the present study, pure and degassed water is employed as a test fluid, and experiments are carried out in the following ranges:

length of heated tube: L = 300, 600, and 900 mm
i.d. of heated tube: d = 8 and 10 mm
system pressure: P = 101.3 and 198.5 kPa
liquid level in reservoir (height from the bottom):
L_w = 150 and 350 mm.

3. EXPERIMENTAL RESULTS

Any experiment in the present study starts with preheating the whole water in the system up to a prescribed saturation temperature T_s by auxiliary heaters in the reservoir and direct current heating of the test-tube. After that, the power input to the heated tube is raised stepwise, keeping the water in the reservoir at the prescribed saturation temperature T_s. At each step of power increase, a steady state of wall temperature is confirmed to continue for a sufficiently long time, and in this way, the power input is increased gradually until the onset of CHF.

3.1. *Onset of CHF and wall temperature excursion*

At any steady state of boiling set up in the above-mentioned process of increasing the power input, it has been found that all thermocouples distributed on the heated tube show nearly the same superheat corresponding to each magnitude of heat flux. For example, Fig. 7(a) shows the variation of local wall temperature with time at four different locations ①–④, where z designates the axial distance from the bottom end of the test-tube. In a period before the time represented by a perpendicular line, during which heat flux is kept at 8.51×10^4 W m^{-2}, it can be observed that the tube wall is maintained at nearly the same superheat at the four different locations against the saturation temperature shown by a thick horizontal line T_s.

However, after a stepwise rise of heat flux made at the perpendicular line in Fig. 7(a) to 8.69×10^4 W m^{-2}, no change of wall temperature is seen for a period (about 50 s in this case), then wall temperature at each location of ①–④ falls gradually towards the saturation temperature, and finally a noticeable change of local wall temperature begins abruptly in succession of ③, ②, and ① (accompanied by a minor and temporary variation at ④). Judging from the

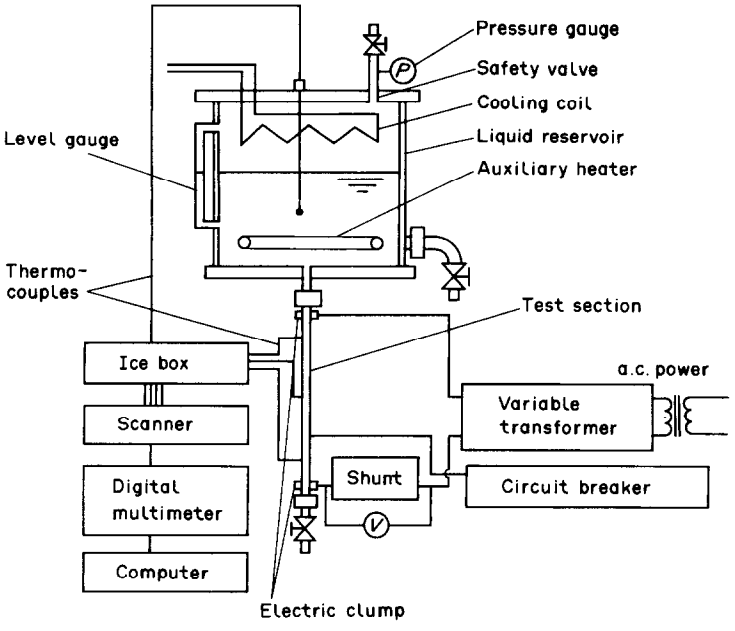

FIG. 5. Experimental apparatus.

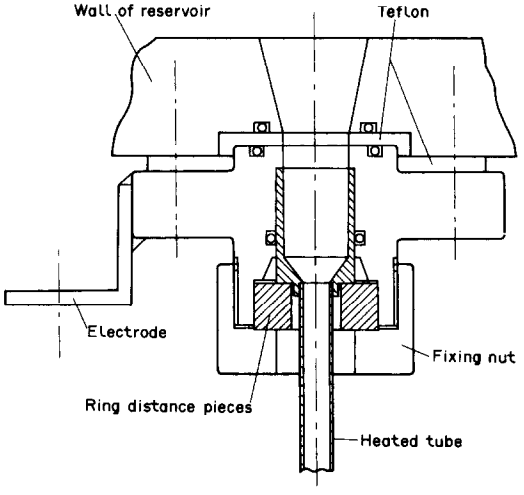

FIG. 6. Structure near the top end of a heated tube.

length of time on the abscissa of Fig. 7(a), the foregoing variation of wall temperature is one which proceeds at a comparatively slow pace.

Figure 7(a) is shown as a typical example, and situations more or less similar to Fig. 7(a) have been observed except for a few cases which display a somewhat simpler type of temperature variation such as that shown in Fig. 7(b).

Finally, as a common fact to Figs. 7(a) and (b), it must be noted that, thermocouples at the locations other than those indicated in Fig. 7(a) or (b) exhibit no temperature variation during the time represented in Fig. 7(a) or (b), being kept at nearly the same superheat.

3.2. *Characteristics of critical heat flux*

In the present study, the critical heat flux q_c is defined as the magnitude of heat flux to bring about noticeable temperature variation in such a way as in Figs. 7(a) and (b); and all the data of q_c thus obtained are plotted in Figs. 8(a) and (b), for $P = 101.3$ and 198.5 kPa, respectively. In Fig. 8, three typical correlations are compared with the data, where 'Nejat' represents q_c predicted by equations (3) and (4); similarly, 'Imura *et al.*' by equation (7); and 'Tien–Chung' by equation (6) with $c_k^2 = 3.2$, respectively.

From the results of Figs. 8(a) and (b), it is noticed that the data of critical heat flux q_c obtained in the present study appear near the prediction line of the Tien–Chung correlation, and that the effect of the liquid level in the reservoir L_w on CHF is negligibly small within the experimental range at least.

3.3. *Location of the onset of CHF*

In the present study, the location of the onset of CHF (measured by the distance from the bottom end of the heated tube $z = L_c$) is defined as the location where the first temperature rise begins, such as ③ of Fig. 7(a) or ② of Fig. 7(b); and all the data of L_c thus obtained are plotted in Figs. 9(a) and (b), for the liquid level in the reservoir $L_w = 150$ and 350 mm, respectively.

The location of the onset of CHF L_c determined in the above-mentioned way has a certain measure of scattering in the nature of things. In spite of this, however, it can be noticed from Figs. 9(a) and (b) that the location of the onset of CHF lies between the top and the bottom end of the heated tube with a tendency to move towards the top end as the tube

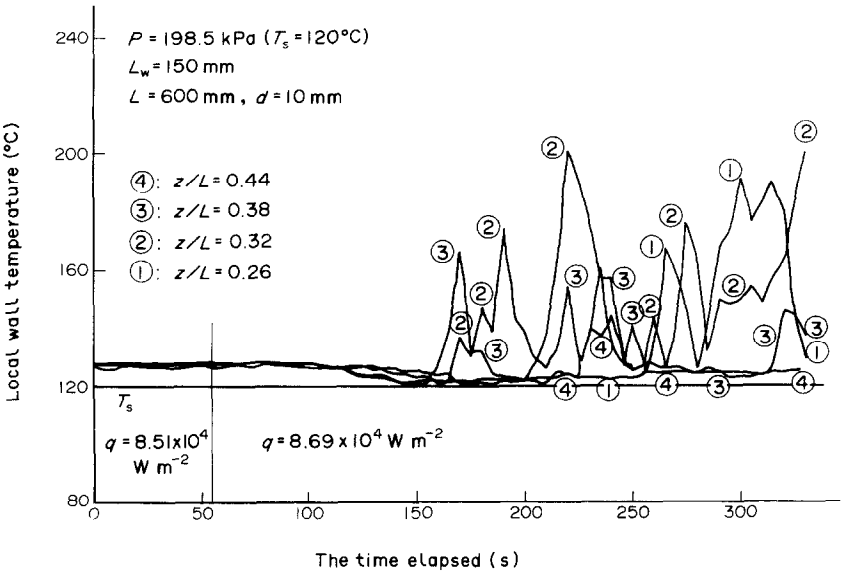

FIG. 7(a). Variation of local wall temperature with time (typical case).

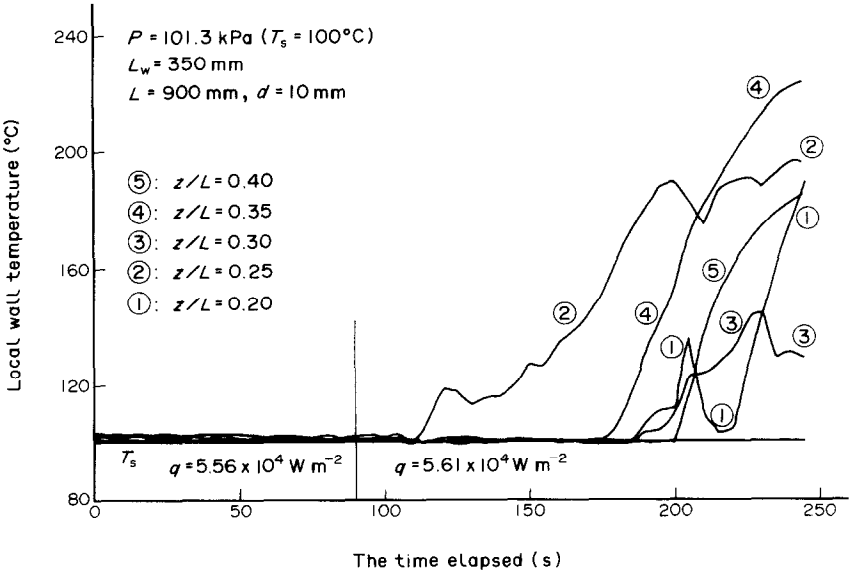

FIG. 7(b). Variation of local wall temperature with time (occasional case).

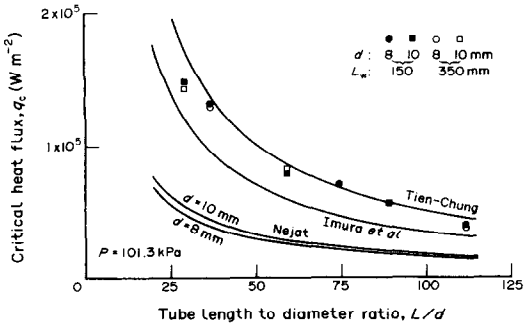

FIG. 8(a). Comparison of measured and predicted CHF (P = 101.3 kPa).

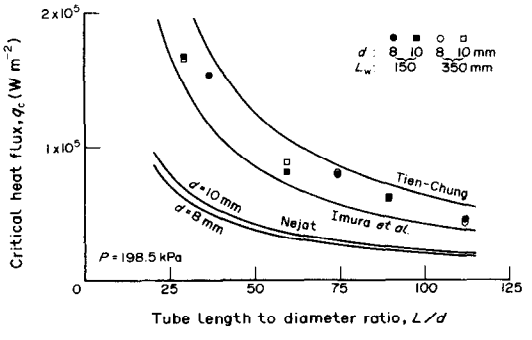

FIG. 8(b). Comparison of measured and predicted CHF (P = 198.5 kPa).

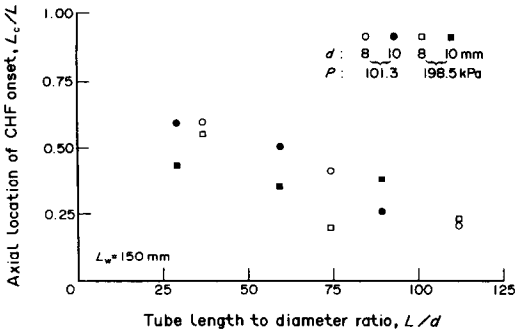

FIG. 9(a). Location of the onset of CHF (L_w = 150 mm).

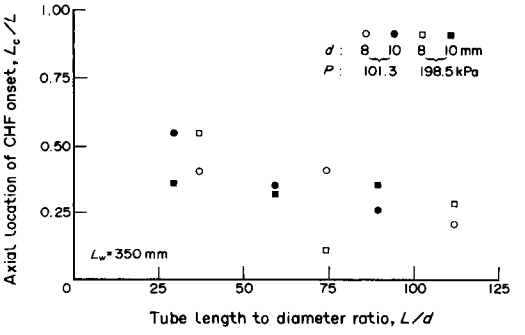

FIG. 9(b). Location of the onset of CHF (L_w = 350 mm).

length is reduced. It is of interest to know that this is in accord with the result of Fig. 3 of Barnard *et al.* [10]. Besides, the fact that Sakhuja [2] reported the onset of CHF at the top end of the heated tube (see the ninth column in Table 1) is also consistent with the foregoing tendency if it is considered that his experiments were made for very short tubes only ($L/d = 2.1$–7.4).

Finally, it is also noticed from Figs. 9(a) and (b) that the presumption of Barnard *et al.* [10] for CHF to arise at the bottom end of a heated tube if the tube is sufficiently long (see Fig. 4(a)), is unrealized up to $L/d = 125$.

4. PHYSICAL SITUATION TO CAUSE CHF

4.1. *Flow pattern model in a heated tube*

For all the data of q_c mentioned in the preceding chapter (for which vapor/liquid density ratio $\rho_v/\rho_L = 0.000623$–0.00119), the superficial velocity of vapor flowing out of the top end of the heated tube j_v at the onset of CHF is calculated by equation (2) to show the following state of high velocity:

$$j_v = 12.6\text{–}15.5 \text{ m s}^{-1} \quad \text{for } P = 101.3 \text{ kPa}$$

$$j_v = 7.8\text{–}9.6 \text{ m s}^{-1} \quad \text{for } P = 196.5 \text{ kPa}.$$

In addition, if q_c is roughly approximated by equation (6) according to the results of Figs. 8(a) and (b), the following equation is derived from equation (2):

$$j_v = c_k^2 \left[\frac{\sigma g(\rho_L - \rho_v)}{\rho_v^2}\right]^{1/4} \Big/ [1 + (\rho_v/\rho_L)^{1/4}]^2 \qquad (8)$$

which suggests that j_v is not affected noticeably by L and d within the experimental range of the present study. It thus appears that one can assume annular counter-flow near the top end of the heated tube just before the onset of CHF.

Meanwhile, for the steady-state boiling in a uniformly heated tube, the upward flow rate of vapor at a location of distance z from the bottom end of the tube (which is equal to the downward flow rate of liquid at the same location) is in proportion to z. Then, the flow rate of vapor near the bottom end of the tube is very low because of $z \cong 0$, and hence one can assume a kind of bubbly flow near the bottom end filled with plenty of liquid.

After all, a distribution of flow patterns along the tube such as that illustrated in Fig. 4(b) can be assumed to appear in a tube just before the onset of CHF. In appearance, this may look very similar to the situation of ordinary forced-flow boiling in a heated vertical tube, but liquid flows opposite to vapor in the present case, causing quite a different situation with respect to the onset of CHF.

4.2. *Location of the onset of CHF and time-lag*

When heat flux is raised to a critical value under the state of Fig. 4(b), it is natural to expect that dryout occurs near a point C because of the minimum thickness of liquid film. Besides, the reduction of liquid film thickness up to zero (that is dryout) near point C is consistent with an experimental fact that wall temperature falls towards saturation temperature just before the onset of abrupt temperature rise (see Figs. 7(a) and (b)). In addition, the above-mentioned situation for the onset of dryout near point C is also consistent with another experimental fact that the location to initiate CHF always lies between the top and the bottom end of a heated tube (see Figs. 3 and 9).

However, it must be remembered that under the steady-state condition, the liquid film at point C in Fig. 4(b) has a flow rate as much as that to compensate for the dissipation of liquid due to evaporation in the region below point C. This means that while the steady state is maintained, the liquid film at point C always has a finite value of flow rate, and besides, the value tends to increase with increasing heat flux if location C is fixed. Hence, in order for dryout to appear near point C under such circumstances, it needs the occurrence of a phenomenon capable of making the inflow rate of liquid less than the outflow rate of vapor at the top end of the heated tube.

Now, according to the results of Figs. 8(a) and (b), it seems to be within the bounds of possibility that a phenomenon such as flooding serves as a trigger to cause CHF in the present boiling system. In addition, when such a phenomenon brings about some

reduction of the inflow rate of liquid at the top end of the heated tube, it needs a finite length of time until dryout is brought about near point C; and this may probably be the cause of a time-lag observed before the onset of wall temperature variation in Fig. 7.

4.3 *Shift of dryout area within a restricted region and slow temperature variation*

The annular counter-flow region near point C in Fig. 4(b) adjoins to a churn or slug flow region existing in the lower part. Consequently, the flow of liquid film in this transition area is rather complicated with a possibility of causing unsteady variation of flow situation. In addition, the situation that plenty of liquid exists in such a way near the dryout area, may probably cause significant heat conduction through the tube wall from the dryout area of high temperature to the lower part of saturation temperature, intensifying nucleate boiling in the lower region.

The above-mentioned situation near point C must exert an influence on the phenomena observed in Fig. 7(a) such as the shift of dryout area within a restricted region near point C and the complicated mode of wall temperature variation. However, as has already been mentioned in Section 3.1, the temperature variation is of a comparatively slow mode in the present case as against a very rapid mode in the case of ordinary CHF. Therefore, in order to offer a more sufficient explanation of the state of Fig. 7(a), it may be necessary to consider additional phenomena such as the fluctuation of the flow rate of liquid from the reservoir to the heated tube. Be the matter as it may, however, the phenomenon described in the Introduction as the oscillation of wall temperature [7] has no connection with the state of Fig. 7(a), which is clear because of quite different nature.

5. CONCLUSIONS

In order to clarify the fundamental nature of CHF phenomenon of boiling in a heated vertical tube with a closed bottom, an experimental study has been carried out in the range of $\rho_v/\rho_L = 0.000623$–0.00119 for the boiling system of Fig. 1(b) with saturated liquid in the reservoir as well as a uniformly heated tube, leading to the following conclusions.

(1) In this boiling system, the location of the onset of CHF lies between the top and the bottom end of the heated tube even for tubes as long as $L/d = 125$, with a tendency to move towards the top end with decreasing L/d.

(2) When heat flux is raised to the critical value from a little lower value, a length of time-lag with no change of wall temperature, and a subsequent period for falling of wall temperature towards saturation temperature are observed until the temperature excursion mentioned in (1) is initiated abruptly. In addition, the temperature variation after the onset of CHF has a slow and complicated mode which is considerably different from that of the ordinary CHF.

(3) Characteristics of CHF mentioned in (1) and (2) make it difficult to detect the onset of CHF in this boiling system correctly. In other words, it requires much circumspection to get accurate data of CHF in this boiling system as against the case of ordinary boiling system.

(4) Even when there is plenty of saturated liquid in the upper reservoir, the state of two-phase flow such as that of Fig. 4(b) appears just before the onset of CHF. In addition to this, if it is assumed that a reduction of the inflow rate of liquid occurs at the critical heat flux q_c due to a phenomenon such as flooding or the like (entrainment of droplets, for example), then the onset of CHF with characteristics mentioned in (1) and (2) can be explained.

(5) It is well known for forced flow boiling in a sufficiently long tube that CHF occurs as a consequence of the dryout of the liquid film in the annular flow region, which is brought about through hydrodynamic process such as entrainment and deposition of droplets. Meanwhile, it can be assumed for the present boiling system that CHF occurs as a consequence of the dryout of liquid film in the annular flow region, which is caused by the hydrodynamic processes such as flooding or the like.

Acknowledgment—The financial support given by Nihon University Research Grants for 1989 to this study [General Individual Research] is gratefully acknowledged.

REFERENCES

1. H. Cohen and F. J. Bayley, Heat-transfer problems of liquid-cooled gas-turbine blades, *Proc. Instn Mech. Engrs* **169,** 1063–1074 (1955).
2. R. K. Sakhuja, Flooding constraint in wickless heat pipes, ASME Paper 73-WA/HT-7 (1973).
3. H. Suematsu, K. Harada, S. Inoue, J. Fujita and Y. Wakiyama, Heat transfer characteristics of heat pipes, *Heat Transfer—Jap. Res.* **7**(1), 1–22 (1978).
4. K. Fukui, J. Sato, M. Hashimoto, M. Munekawa and A. Furusawa, Heat transfer characteristics of heat pipes of thermosyphon type, *Prepr. Japan Soc. Mech. Engrs* No. 790-18, 143–145 (1979).
5. K. Harada, S. Inoue, J. Fujita, H. Suematsu and Y. Wakiyama, Heat transfer characteristics of large scale heat pipes, *Hitachi Zosen Tech. Rev.* **41,** 167–174 (1980).
6. H. Imura, K. Sasaguchi and H. Kozai, Critical heat flux in a closed two-phase thermosyphon, *Int. J. Heat Mass Transfer* **26,** 1181–1188 (1983).
7. T. Fukano, S. J. Chen and C. L. Tien, Operating limits of the closed two-phase thermosyphon, *ASME–JSME Thermal Engng Joint Conf. Proc.*, Vol. 1, pp. 95–101 (1983).
8. T. Fukano, K. Kadoguchi and C. L. Tien, Oscillation phenomena and operating limits of the closed two-phase thermosyphon, *Proc. 8th Int. Heat Transfer Conf.*, Vol. 5, pp. 2325–2330 (1986).
9. T. Fukano, K. Kadoguchi and H. Imuta, Experimental study on the heat flux at the operating limit of a closed two-phase thermosyphon, *Trans. JSME* **53(B),** 1065–1071 (1987).
10. D. A. Barnard, F. R. Dell and R. A. Stinchcombe,

Dryout at low mass velocities for an upward boiling flow of Refrigerant-113 in a vertical tube, UKAEA, AERE-R 7726 (1974).
11. Z. Nejat, Effect of density ratio on critical heat flux in closed end vertical tubes, *Int. J. Multiphase Flow* **7**, 321–327 (1981).
12. Ye. L. Smirnov, Critical heat flux in flooding in vertical channels, *Heat Transfer—Sov. Res.* **16**(3), 19–24 (1984).
13. F. Dobran, Steady-state characteristics and stability thresholds of a closed two-phase thermosyphon, *Int. J. Heat Mass Transfer* **28**, 949–957 (1985).
14. J. G. Reed and C. L. Tien, Modeling of the two-phase closed thermosyphon, *Trans. ASME, J. Heat Transfer* **109**, 722–730 (1987).
15. C. Casarosa and F. Dobran, Experimental investigation and analytical modeling of a closed two-phase thermosyphon with imposed convection boundary conditions, *Int. J. Heat Mass Transfer* **31**, 1815–1833 (1988).
16. S. G. Bankoff and S. C. Lee, A critical review of the flooding literature. In *Multiphase Science and Technology* (Edited by G. F. Hewitt, J. M. Delhaye and N. Zuber), Vol. 2, pp. 96–180. Hemisphere, Washington, DC (1986).
17. G. B. Wallis, Flooding velocities for air and water in vertical tubes, UKAEA, AEEW-R 123 (1961).
18. J. E. Diehl and C. R. Koppany, Flooding velocity correlation for gas–liquid counterflow in vertical tubes, *Chem. Engng Prog. Symp. Ser.* **65**, 77–83 (1969).
19. M. K. Bezrodnyi, The upper limit of maximum heat transfer capacity of evaporative thermosyphons, *Teploenergetika* **25**, 63–66 (1978).
20. C. L. Tien and K. S. Chung, Entrainment limits in heat pipes, *AIAA J.* **17**, 643–646 (1979).
21. Y. Katto, Critical heat flux. In *Advances in Heat Transfer* (Edited by J. P. Hartnett and T. F. Irvine, Jr.), Vol. 17, pp. 1–64. Academic Press, New York (1985).

FLUX THERMIQUE CRITIQUE DE L'EBULLITION DANS UN CONTRE-COURANT A L'INTERIEUR D'UN TUBE VERTICAL CHAUFFE AVEC UNE BASE FERMEE

Résumé—On présente une étude expérimentale du flux thermique critique (CHF) de l'ébullition dans un contre-courant à l'intérieur d'un tube vertical chauffé uniformément qui est ouvert en haut sur un grand réservoir de liquide et est fermé à sa base. Les caractéristiques CHF sont complètement différentes de celles dans un système ordinaire en ce qui concerne la position du CHF initial dans le tube, le délai notablement distinct, une période plus importante de chute de la température pariétale locale juste avant l'apparition du CHF et la variation plus compliquée et comparativement plus lente de la température pariétale locale après l'apparition du CHF. Un modèle physique est discuté pour l'explication de ces phénomènes très particuliers par le comportement de la vapeur et du liquide dans le tube chaud.

KRITISCHE WÄRMESTROMDICHTE BEIM SIEDEN IN GEGENSTRÖMUNG IN EINEM GLEICHFÖRMIG BEHEIZTEN, SENKRECHTEN ROHR MIT GESCHLOSSENEM BODEN

Zusammenfassung—Die kritische Wärmestromdichte (CHF) beim Sieden in Gegenströmung in einem gleichförmig beheizten, senkrechten Rohr wird experimentell untersucht. Das Rohr ist am unteren Ende verschlossen und geht am oberen Ende in einen großen Flüssigkeitsbehälter über. Die wichtigsten Erkenntnisse sind: das beschriebene System verhält sich beim Erreichen des CHF grundsätzlich anders als übliche Siedesysteme; dies trifft in besonderer Weise auf die Stelle im Rohr zu, an welcher CHF zuerst auftritt; vor dem Eintreten des CHF ist über ein bestimmtes Zeitintervall ein Absinken der örtlichen Wandtemperatur zu beobachten; nach dem Auftreten des CHF ändern sich die örtlichen Wandtemperaturen langsam in komplizierten Verläufen. Abschließend wird ein physikalisches Modell zur Beschreibung dieser besonderen Phänomene mit Hilfe des Verhaltens von Dampf und Flüssigkeit in einem beheizten Rohr diskutiert.

КРИТИЧЕСКИЙ ТЕПЛОВОЙ ПОТОК ПРИ КИПЕНИИ В УСЛОВИЯХ ВСТРЕЧНЫХ ТЕЧЕНИЙ В РАВНОМЕРНО НАГРЕВАЕМОЙ ВЕРТИКАЛЬНОЙ ТРУБЕ С ЗАМКНУТЫМ НИЖНИМ ТОРЦОМ

Аннотация—Экспериментально исследуется критический тепловой поток (КТП) при кипении в условиях встречных течений в равномерно нагреваемой вертикальной трубе, открытый верхний торец которой сообщается с большим резервуаром жидкости, а нижний замкнут. Выявлены характеристики КТП, в рассматриваемом случае значительно отличающиеся от случая с обыкновенной системой кипения, а именно, место возникновения КТП в трубе, существенное время запаздывания и последующий период падения локальной температуры стенки непосредственно перед началом КТП, а также сложное и сравнительно медленное изменение локальной температуры стенки после возникновения КТП. Обсуждается физическая модель, позволяющая объяснить эти специфические явления на основе поведения пара и жидкости в нагреваемой трубе.